CNPq

CBPF - CENTRO BRASILEIRO DE PESQUISAS FÍSICAS

Notas de Física

CBPF-NF-028/92

STUDY ON COSMIC RAY INTERACTIONS IN THE ENERGY REGION $\Sigma E_{\gamma} > 1000$ TeV

by

N. AMATO, E. SHIBUYA, R.H.C. MALDONADO,
and H.M. PORTELLA

ABSTRACT

To study the typical aspects of the phenomena in the super high energy region, that will be the main energy region of interest of the next experiments using nuclear emulsion chamber, we took the data of the superfamilies of Brazil-Japan Collaboration and compared them with experimental detailed information of an event with ΣE_{γ} >1000 TeV of the same Collaboration. These superfamilies were also compared with simulated families using different primary composition (P, CNO, Fe) and Scaling-type interaction. In the correlation between hadrons and gamma rays we observed that some events were situated in the simulation region where the primaires were identified as heavy primaries. These events can be explained as Centauro type due to their big values of the hadronic number and the hadronic energy. The others events were situated either in the intermediary region or in the region that correspond to proton primary. Then there is a variety of superfamilies.

Key-words: Cosmic ray; Emulsion chamber; Halo events.

PACS 96.40 DE, 13.85 TP.

1 INTRODUCTION

The region of energy $\Sigma E_\gamma > 1000$ TeV is called "superhigh energy" and the events in this region are called "superfamilies"[1]. Through the study of high energy A-jets detected by nuclear emulsion chamber exposed in altitude of mountain, it is possible to obtain informations on Cosmic Ray Phenomena beyond the domain reached by the recent accelerators and that has been studied so far only by extensive air showers (EAS) experiments[2].

It is important to consider, as great advantages, the fact that the nuclear emulsion chamber experiment in altitude mountains can provide the details of the events which can not be obtained by EAS experiments.

Up to now the Brazil-Japan Collaboration has published the results on six superfamilies: Andromeda[3,4,5], Ursa Maior[4,5], M.A.I[4], M.A.II[4], M.A.III[4], PO6[6] and more two preliminary results on C18S86[7] and C21S87175[8]. These events are associated with a generally darkened area of X-ray films in the central region, which is called "halo". The events associated with halos are called the "Halo events". This central region on the target diagram corresponds to the very forward angular region in general.

The experiments at Pamir[9], Mt. Fuji[10], Kanbala[11] and Tien Shan[12] have also observed "Halo events". Thus it can be said that the appearance of a strong concentration of energy as a halo is a rather common feature in the superhigh energy region.

The study of the different aspects on the Halo events is important to understand the phenomena of collision in the high energy region.

In this paper are presented the results obtained from analysis on

P06 event and a comparison with those obtained on three superfamilies detected in Chacaltaya: Andromeda, Ursa Maior and M.A.III.

Two different methods used on A-jets analysis were applied in these superfamilies: Simulation and Decascading.

For the Simulation calculation we made the assumptions of proton primary, constant interaction cross section and scaling type interaction based on others simulations[13,14] which showed that the efficiency of heavy primary for criation of halo events is lower, by a factor 10 or more, than that of the proton primary and that the scaling model give a concentration of particles and energy in the forward angular region larger than those obtained by scaling violation.

It was made a comparison with the results on simulation calculation obtained by Yamashita[5] including heavy primaries. For Decascading procedure we used the Semba method[15].

2 RESULTS

Table 1 presents the results of the event P06, using a special method of analysis[6], together with those of others three families: Andromeda, Ursa Maior and M.A.III.

Fig. 1 show the integral spectra of energy of gammas and electrons of P06 and the others superfamilies. The spectra are presented in the form $f_\gamma = E_\gamma / \Sigma\Sigma_\gamma$ which permit to compare families of different ΣE_γ.

We observed a general similarity between these spectra, although the spectrum of P06 shows a deviation from the power form.

Fig. 2 shows the similar spectra of hadrons for these families. When we compare the spectra of different components we observe that the spectra of hadronic part are softer than those of the electromagnetic ones; so the contribution of particles with high energy is larger for the hadronic than for the electromagnetic component.

This situation becomes clear in the Fig. 3 that presents the exponents β_γ and β_h of both power spectra. These exponents were calculated in the region of energy above the value E_c through the expression: $1/\beta=<\ell n (E/E_c)>$, where E_c is the energy chosen for cut.

The values of E_c (in TeV) are showed in the respective points of the figure.

The exponents were considered in the region where the number of particles was larger than 10 to obtain a significant statistic, but for PO6, which had few hadrons, we considered the region where the number of particles was 7.

We observe that for the three families: Andromeda, Ursa Maior and M.A.III the β_γ is always larger than β_h and the difference increases when the energy increases. For the PO6 we do not observe any difference between these power indices.

These indices give an idea of the cascade process in the atmosphere. In this way it is possible to say that the hadronic component is still young while the electromagnetic component is becoming old for the events Andromeda, Ursa Maior and M.A.III. For the PO6 event the espectrum of energy is almost exponential; it is possible then that the equality between β_γ and β_h is indicating that the gamma rays are also still young.

3.1 Decascading

Frequently we find groups of showers in the family coming from gamma rays and electrons that developed cascades in the atmosphere before arriving the nuclear emulsion chamber. The decascading procedure using K=12 TeVmm[15], was applied in these families in order to find such groups of showers and to substitute them by the original gamma rays, which are called "decascaded gamma rays".

This procedure gives information about the original gamma rays in the nuclear atmospheric interaction.

Fig. 4 shows the diagram of E_γ^* and R_γ^* for decascaded gamma rays of the P06 and of the others three families.

We observe that the points fall in the line ER=constant. This is due to the general tendency of P_T=constant for the original gamma rays.

The values of $\langle E_\gamma^* R_\gamma^* \rangle$ for these families are presented in the Table 2. For the families of lower energy ΣE_γ=100-1000 TeV, the value of $\langle E_\gamma^* R_\gamma^* \rangle$ is situated in the interval (150-500 TeV). Thus we did not observe a large difference between the decascaded gamma rays of the superfamilies and the gamma rays of the lower energy families.

To find the gamma rays and electrons that were originated from the same jet we applied the decascading procedure to the decascaded gamma rays using the value K=250 TeVmm[16].

Fig. 5 shows the jets that were obtained for the P06 event, and for the others families. In this figure E_j represents the total energy of the decascaded gamma rays of a jet and R_j is the distance of the center of the energy of the jet to the center of the family.

The value of $\langle E_j R_j \rangle$ for the PO6 event is also presented in the Table 2 together with the results of the others three families. In this Table is also presented the value obtained in the lower energy families ΣE_γ=(100-1000) TeV. We observe that this value is small when compared with those of the four families.

3.2 Main interaction as halo origin

We suppose that the halo part comes from the main interaction in the nuclear and electromagnetic cascade process. Then we try to understand the characteristics of the "halo". For this, we make, for the PO6 event the sum of the energy of the particles inside the interval Δ (log R), where R is the distance to the center of the family. Fig. 6 shows the lateral distribution of the energy density of the eletromagnetic component for the PO6 event and for the others families.

Only gamma rays with E>2 TeV were considered. We observe that in the PO6, Ursa Maior and M.A.III the distributions present a enhanced peak for small R and a large tail for large values of R. Knowing that for a given value of the mass of the fireball M_γ the quantity $\Sigma E_\gamma R_\gamma$ becomes constant when the height of the interaction is larger than 100m we take the variable $R_c \Sigma E$ ($R<R_c$) as a measure of the lateral spread (wheigted in energy) of the halo part, where R_c and ΣE ($R<R_c$) represent, respectively, the distance of the peak of the energy density distribution (that could correspond to the half-angle of the fire ball), and the total energy within this distance (that could correspond to 3/4 of the product $M_\gamma \Gamma$, where M_γ is

the mass of the fireball and Γ is its Lorentz factor). The lateral distributions of the energy density was made also for the simulated families with $\Sigma E_\gamma > 2000$ TeV[5]. Three different examples are presented in the Fig. 7, one for each primary composition: P, CNO and Fe.

We define the lateral spread of the main interaction as the distance, R_c, of the center of the family to the first peak of the distribution of the energy density. Thus we take the $\Sigma E_\gamma (R<R_c)$ as being the energy coming from the main interaction. This quantity was calculated for the P06 event, and presented in Table 3 together the values for the others superfamilies.

Table 3 presents also the values of the lateral spread normalized in energy $R_c \Sigma E_\gamma (R<R_c)$ for the same families.

Table 4 shows the average values for the families obtained through simulation for each primary composition (P, CNO, Fe) using Scaling model (S), with $\Sigma E_\gamma > 2000$ TeV.

Although the statistical errors are big for each model, we observe that the FeS, in this energy region, can not explain the experimental results (the simulated events present a bigger spread). The PS and CNOS models can reproduce the events although the CNOS presents the average value bigger than the real events.

This fact suggests that the characteristics of the particles of the showers inside the halo part can have PS nature. Then this model can be good to search for the special aspects that could appear in the halo part.

3.3 Primary composition

To study the primary composition under the assumption of scaling type interaction, we analysed the PO6 event and the others superfamilies based on the correlation between the energy and particle number released in hadrons and gamma rays separately. To investigate the hadronic characteristic of the halo events, we compared them with the events simulated by Yamashita[5] for different types of composition of primary particles: protons (P), intermediary nuclei (CNO) and heavy nucleus (Fe), under Scaling assumption (S) for nuclear interaction. We compared also with 119 events obtained by Monte Carlo Simulation made under proton primary particle assumption and scaling type interaction[6]. Fig. 8 shows the diagram of total energy for the hadronic component ΣE_h and for the eletromagnetic component ΣE_γ.

Fig. 9 presents a diagram for total number of particles, N_h and N_γ. In these figures the results obtained from the experimental data and from the 119 simulated events were corrected for the detection loss. The results obtained from Yamashita Simulation were selected with $\Sigma E_t = (\Sigma E_\gamma + \Sigma E_h) > 1000$ TeV for the different types of particles.

We observed that the Andromeda and M.A.III were situated in the FeS region, the Ursa Maior event in the intermediary region and PO6 in the PS region.

DISCUSSION AND CONCLUSION

To study the typical aspects of the phenomena in the super high energy ΣE_γ > 1000 TeV, we presented the data of the superfamilies of the Brazil-Japan Collaboration and compared them with detailed information of the P06 event.

These superfamilies with "Halo" were also compared with the families obtained from simulation calculation. From the observation of the position of the halo peak and the energy released inside the halo part we noticed that the halo can be explained assuming proton as primary particle and scaling type interaction. If we suppose that the primary cosmic rays are heavy nuclei, we will obtain the lateral spread weighted in energy bigger than the experimental results.

In the correlation between hadrons and gamma rays, the Andromeda and M.A.III are situated in simulation region where the primaries were considered heavy nuclei.

These events can be Centauro type events, which can give a big value of hadronic energy and hadronic particle number. The Ursa Maior event is situated in the intermediary region while the P06 event is located in the region corresponding to the primary proton. We observed that there is a variety of superfamily types.

ACKNOWLEDGMENTS

The authors thank the members of the Chacaltaya Emulsion Chamber Experiment of the Brasil-Japan Collaboration for their valuable discussions.

FIGURE CAPTIONS

Figure 1 - Fractional energy spectrum of gammas/electrons in integral form

O Andromeda X Ursa Maior

● M.A.III □ PO6

The curve is the average of five families with ΣE_γ=1000-3000 TeV of Mt. Fuji experiment.

Figure 2 - Fractional energy spectrum of hadron in integral form

O Andromeda X Ursa Maior

● M.A.III □ PO6

Figure 3 - Power indices β_γ and B_h of energy spectrum of gamma rays and hadrons in the energy region above E_c.

O Andromeda X Ursa Maior

● M.A.III □ PO6

Figure 4 - Diagram of E_γ^* and R_γ^* of gamma rays decascaded

O Andromeda X Ursa Maior

● M.A.III + PO6

Figure 5 - Diagram of E_{jet} R_{jet}

O Andromeda X Ursa Maior

● M.A.III + PO6

Figure 6 - Lateral distributions of energy density in $\log_{10}$ R scale

a) Andromeda c) Ursa Maior

b) M.A.III d) PO6

Figure 7 - Lateral distributions of energy density of three simulated events.

a) PS (ΣE=1557 TeV)

b) CNOS (ΣE=2217 TeV)

c) FES (ΣE=5495 TeV)

Figure 8 - Diagram of ΣE_{γ} and ΣE_{h}

Δ Andromeda ∇ Ursa Maior

● M.A.III ■ PO6

Δ PS, +CNOS, O FE and o PS

Figure 9 - Diagram of N_{γ} and N_{h}

Δ Andromeda ∇ Ursa Maior

M.A.III ■ PO6

Δ PS, +CNOS, O FE and o PS

TABLE CAPTIONS

TABLE 1: - Experimental results of four families with haio.

TABLE 2: - Values of $\langle E\gamma^{*} R\gamma^{*} \rangle$ and $\langle Ej\ Rj \rangle$ of the four families.

TABLE 3: - Lateral spread of the four families.

TABLE 4: - Average value of lateral spread of simulated families.

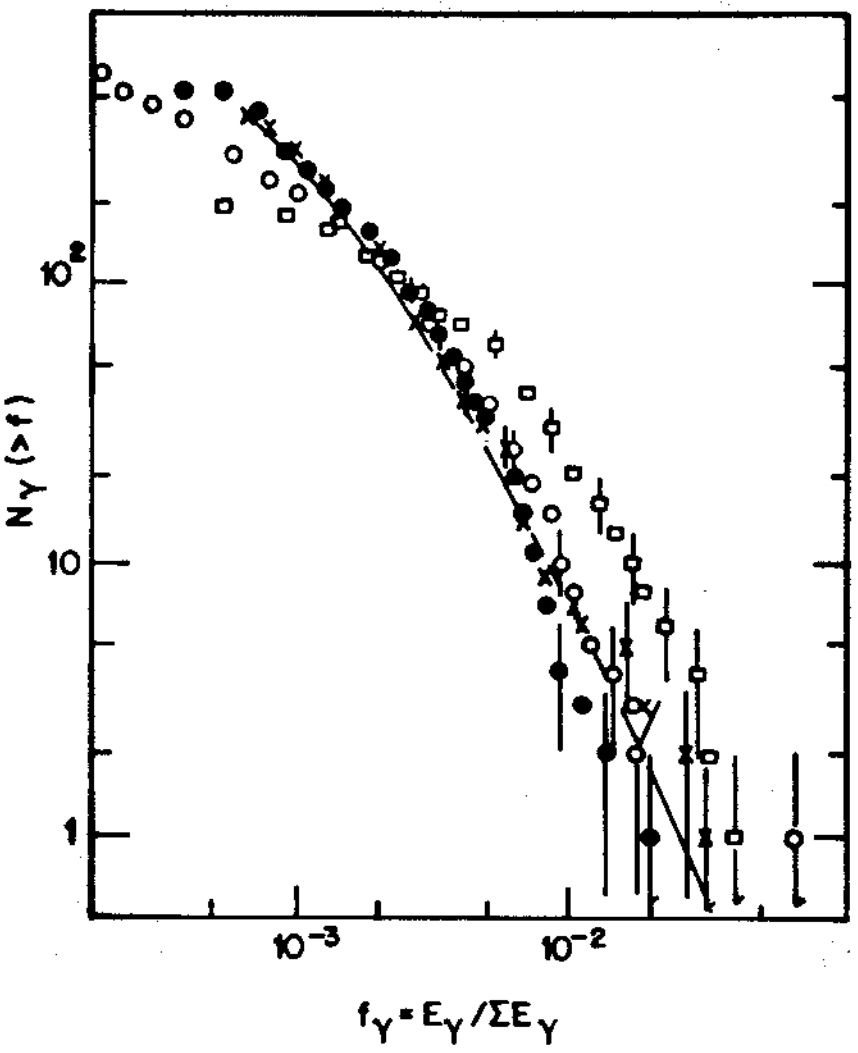

Fig. 1

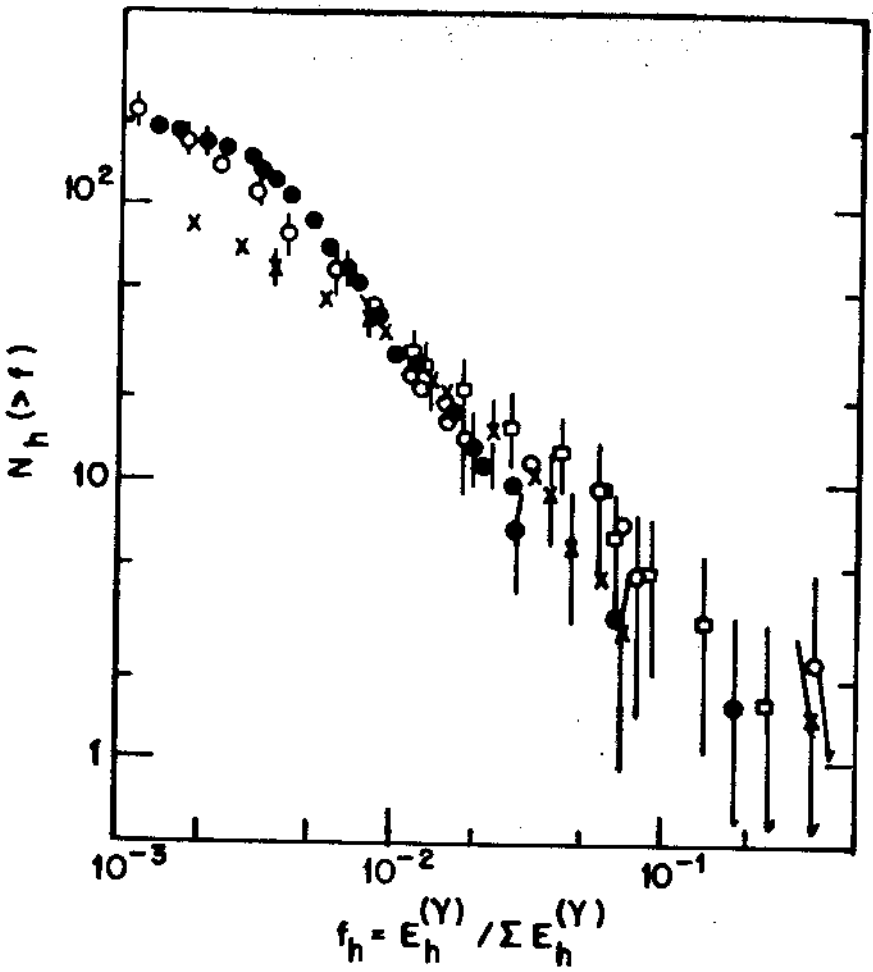

Fig. 2

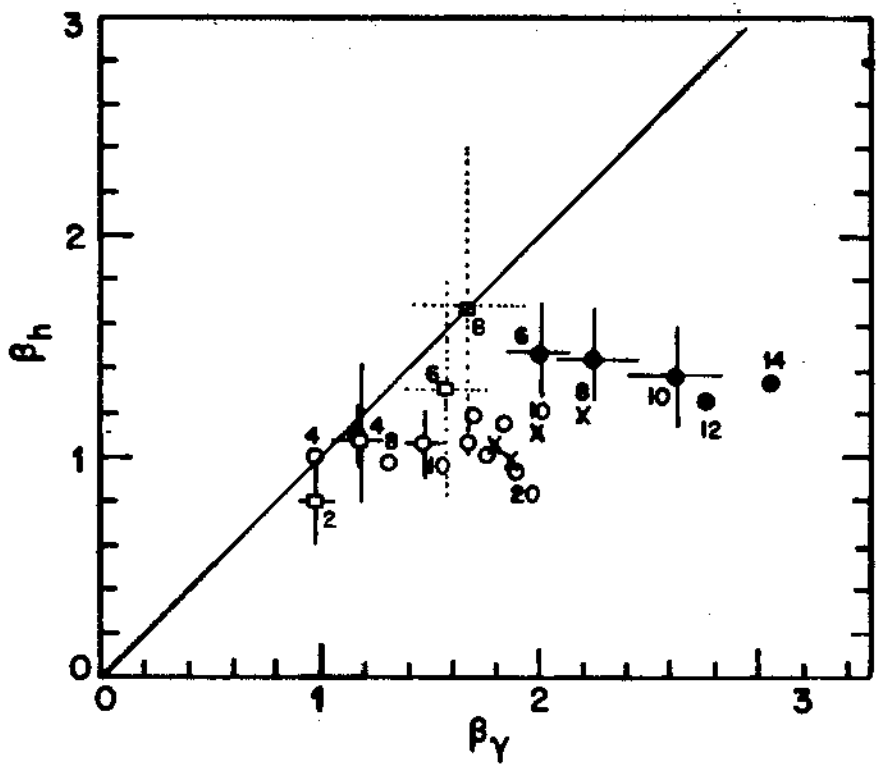

Fig. 3

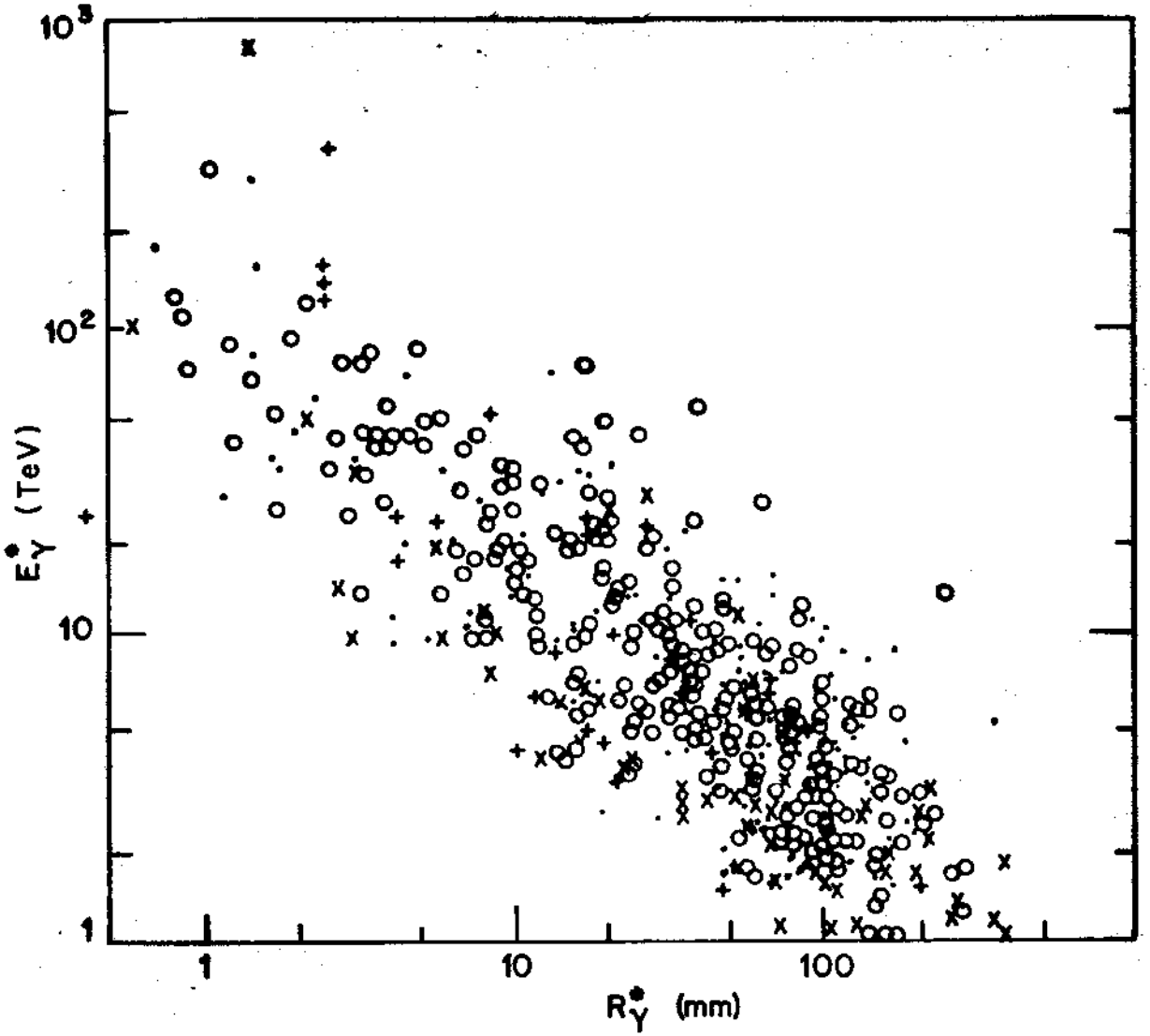

Fig. 4

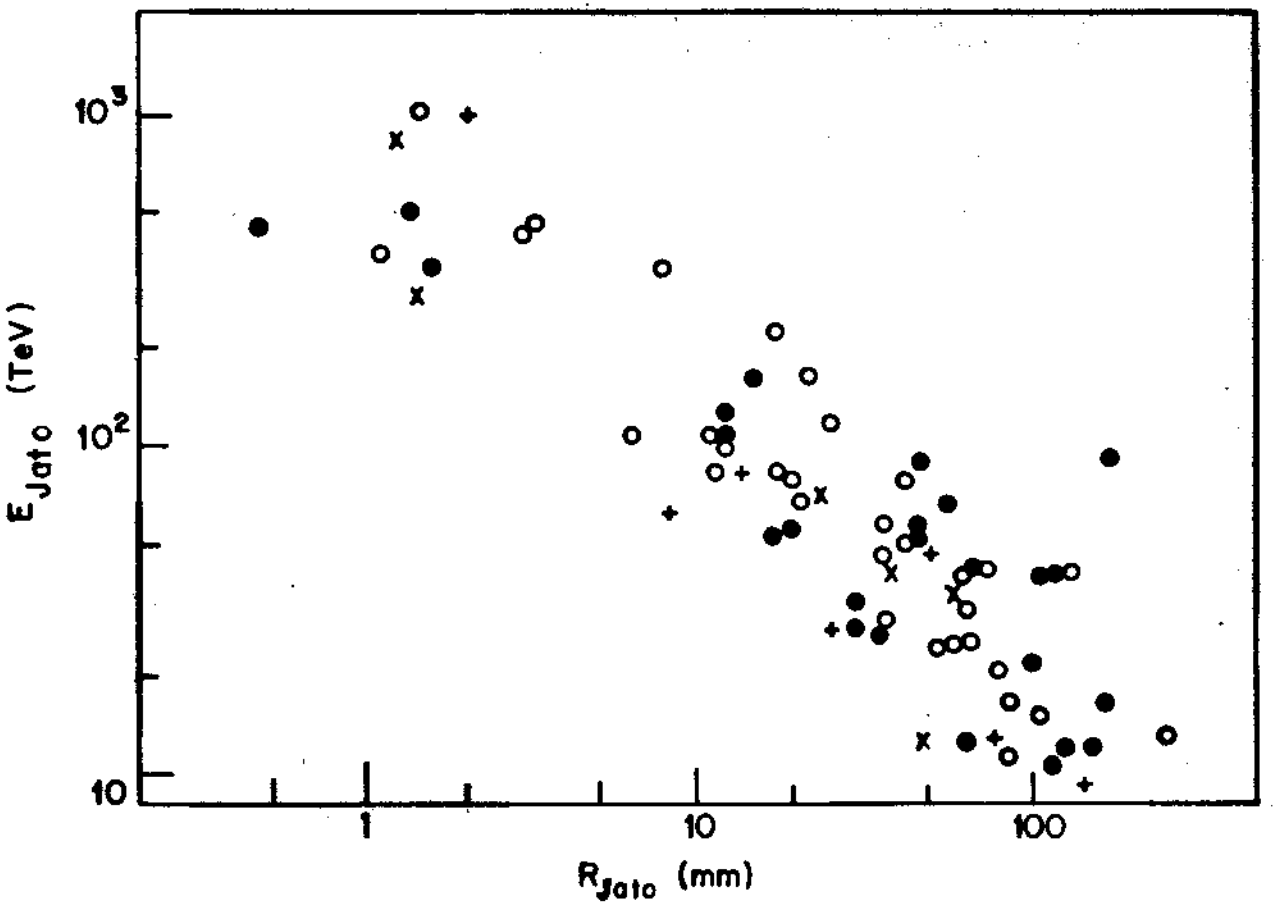

Fig. 5

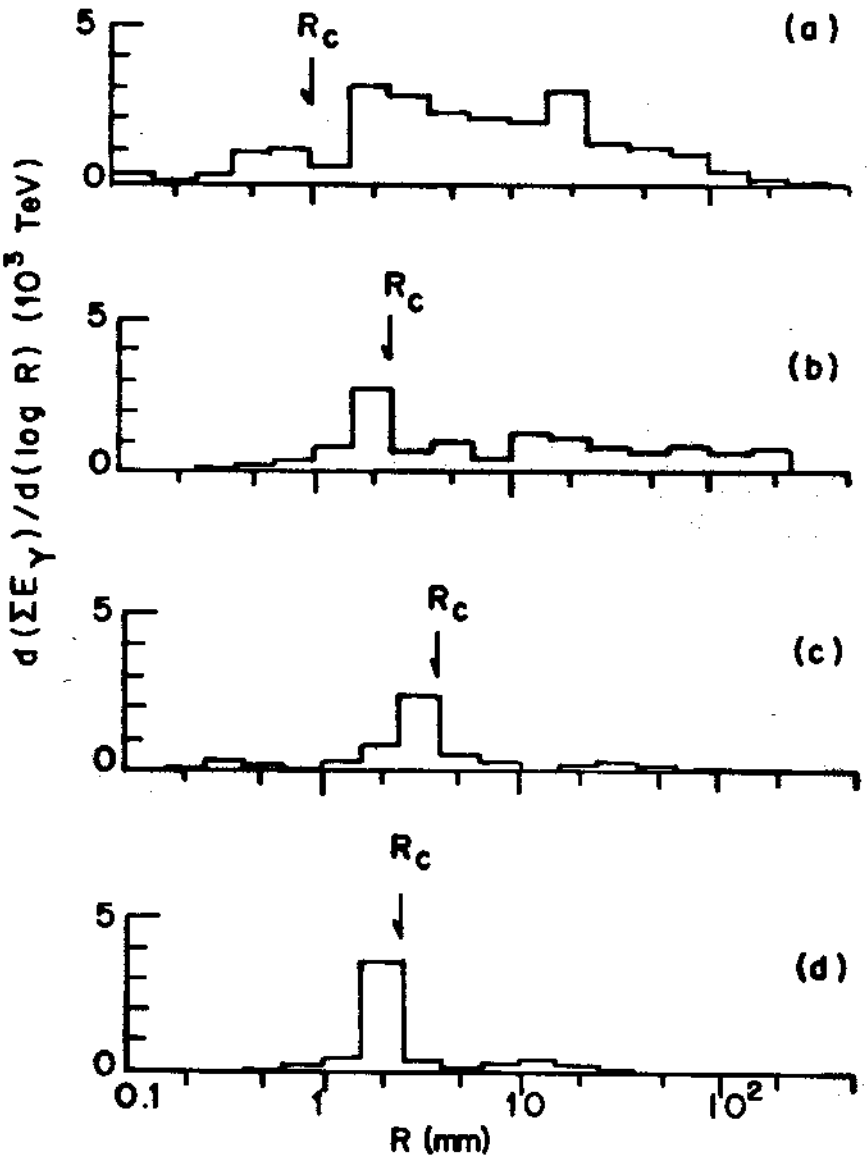

Fig. 6

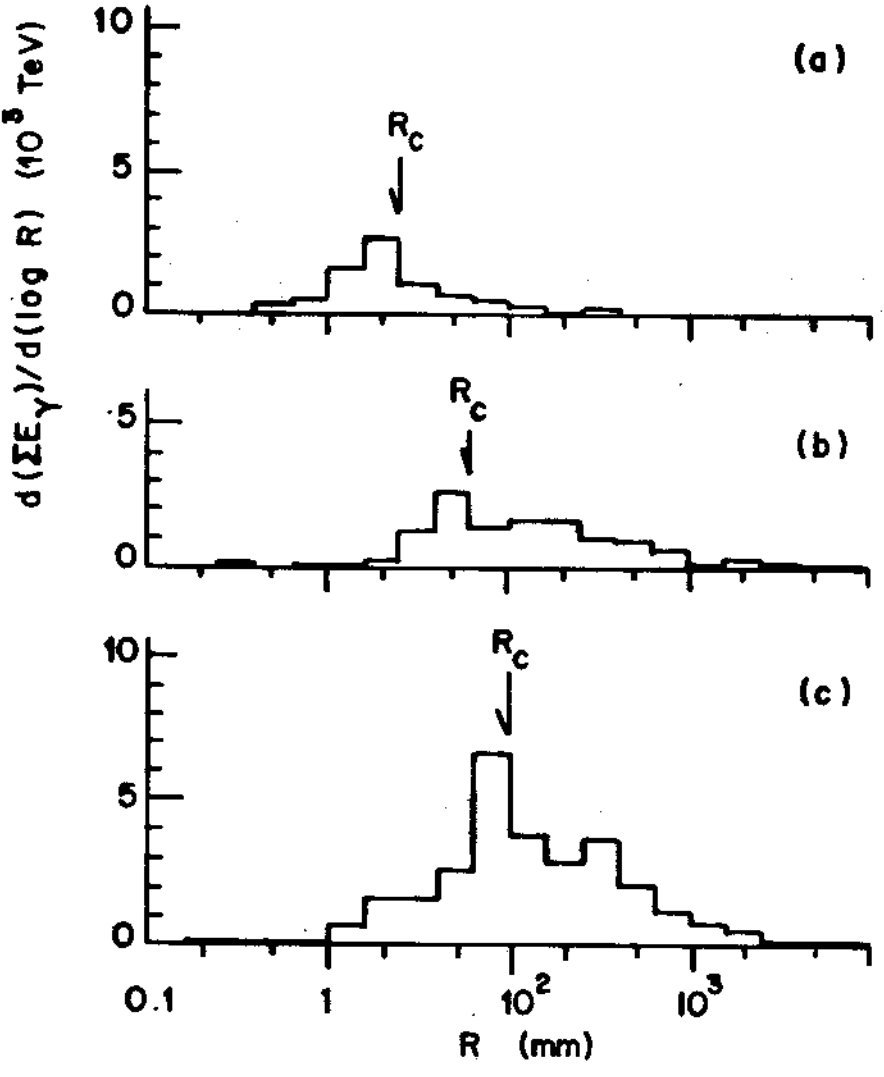

Fig. 7

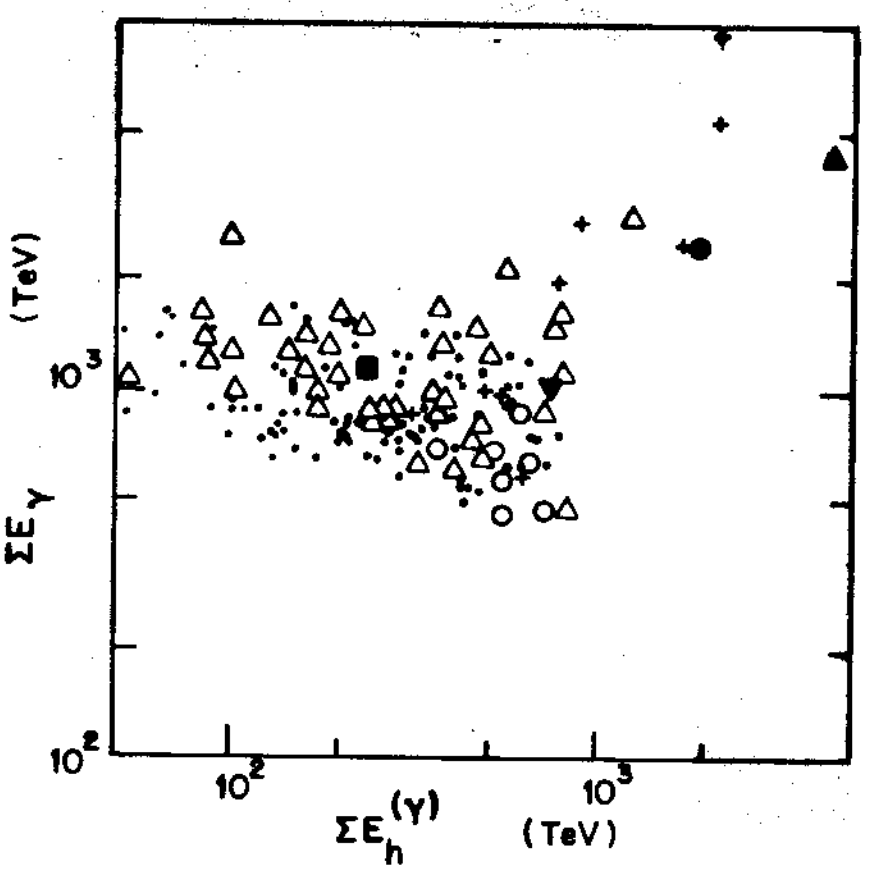

Fig. 8

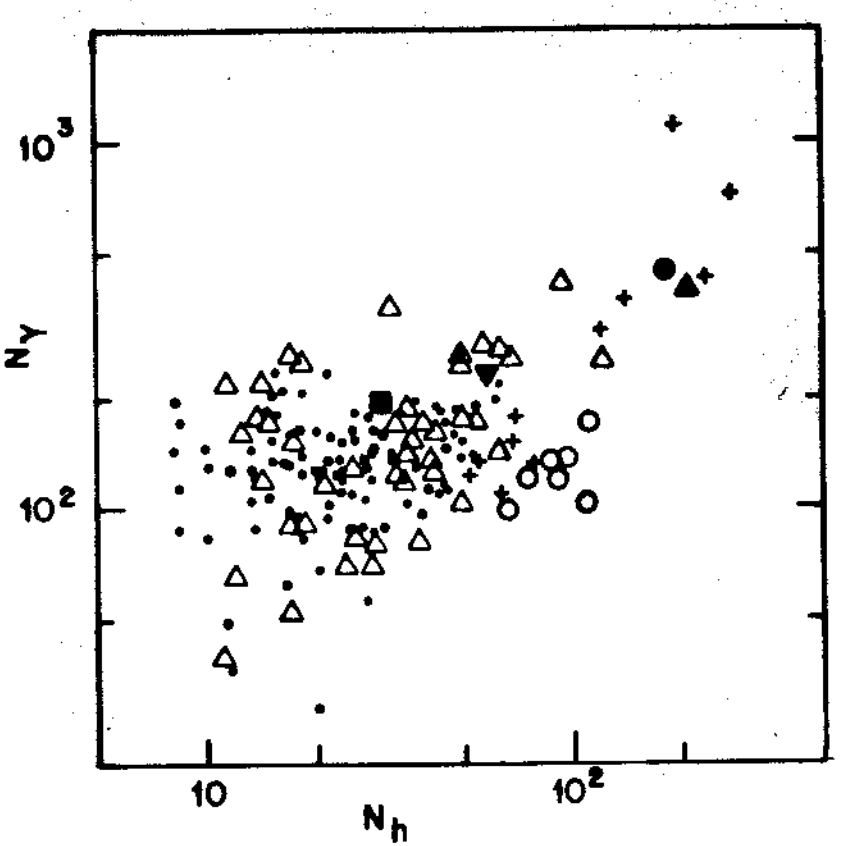

Fig. 9

TABLE 1

Experimental Results of four families with halo				
Name of event	Andromeda	Ursa Maior	M.A.III	P06
Zenithal angle	53	25	49	31
Chamber	C14	C15	C19	C18
HALO				
Radius (cm)	3,2	0,9	2,2	0,65
Total energy (TeV)	21000	980	5100	1043
SHOWERS				
γ/e E_γ >1 TeV				
Multiplicity	627	430	537	191
Total energy (TeV)	4488	1344	2531	1126
hadrons $E_h^{(\gamma)}$ > 1TeV				
Multiplicity	110 (268)	54 (84)	115 (195)	18 (31)
Total energy (TeV)	1656 (4039)	532 (830)	1172 (1986)	143 (243)

TABLE 2

Values of $\langle E\gamma^* R\gamma^* \rangle$ and $\langle Ej\ Rj \rangle$ of four families Descasding	gamma ray	jet
K value (TeV mm)	12	250
Andromeda	360	2100
Ursa Maior	270	1300
M.A. III	480	2600
PO6	300	1340
Families (100-1000)TeV	303	1017

TABLE 3

Name of event	Lateral spread of four families		
	Lateral spread R_c (mm)	Total Energy ΣE_γ (R < Rc) (TeV)	$R\Sigma E$(R < R) (GeV Km)
Andromeda	1,0	323 (7,2%)	0.32
Ursa Maior	4,0	700 (52,1%)	2,8
M.A.III	2,5	796 (31,5%)	2,0
PO6	2,5	813 (79,0%)	2,0

TABLE 4

Average value of lateral spread of simulated families	
model	$R\Sigma E_\gamma (R > R_c)$ (GeV Km)
PS	2,7 + 0.8
CNOS	6,6 + 1.7
FES	19.5 + 4,4

REFERENCES

1. C.M.G. Lattes, Y. Fujimoto and S. Hasegawa, Phys. Rep. **65**, 152 (1980).

2. C.M. Lattes et al Prog. Theor. Phys. Suppl., **47**, 1 (1971).

3. A. Ohsawa, Institute for Cosmic Ray Research, University of Tokyo Report No. **112-836**, 529 (1983.

4. S. Yamashita, J. Phys. Soc. Japan, **54**, 529 (1985).

5. J.A. Chinellato, Doct. Thes-UNICAMP - (1981).

6. N. Amato, N. Arata, R.H.C. Maldonado, Nuovo Cimento **10C**, 559 (1987).

7. K. Sawayanagi, Proceedings of International Simposium on Cosmic Ray and Particle Physics Tokyo (1984), p. 116.

8. J.A. Chinellato et al., Proceendings of International Simposium on Cosmic Ray and Particle Physics, Lodz (1988), p. 309.

9. Pamir Collab., Proceedings of the 18^{th} International Cosmic Ray conference, Bangalore (1983), vol 5, 437.
   A.S. Borisov et al., Proceedings of International Simposium on Cosmic Ray and Particle Physics, Tokyo (1984), p. 3.
   Proceedings of the 20^{th} International Cosmic Ray Conference Moscow (1987), vol. 5, p. 383.

10. J.R. Ren et al. Proceedings of the 20^{th} International Cosmic Ray Conference, Moscow, (1987), vol. 5, p. 371.

11. M. Akashi et al., Nuovo Cim. **67A**, 221 (1982).

12. Chasnikov I. Ya. et al - Proceedings of the 20^{th} International Cosmic Ray Conference, Moscow (1987), vol 5, p. 218.

13. J.R. Ren et al., Proceedings of the 20^{th} International Cosmic Ray Conference, Moscow (1987), vol. 5, p. 375.

14. M. Shibata, Phys. Rev. D24, 1847 (1981).

15 H. Semba, Prog. Theor. Phys. Suppl. 76, 111 (1983).

16. H. Semba, Proceedings of International Simposium on Cosmic Ray and Particle Physics, Tokyo, (1984), p. 211.